Clinical and Translational Science

ARTICLE OPEN ACCESS

A Bayesian-Based Integrative Bioinformatics Analysis Nominates Oncogenic Drivers in Neuroblastoma

Lin Xu[1,2] | Arhanti Sadanand[1] | Evan W. Neczypor[3] | Yen-Ting Liu[1] | Erin Butler[1] | Kelley Moore[4] | Flannery Bowman[5] | Yamin Mazumder[5] | Arlene Naranjo[6] | Alexandre Chlenski[4] | Xue Xiao[2] | Lei Guo[2] | Susan L. Cohn[4] | Mark A. Applebaum[4] | Stephen X. Skapek[5]

[1]Department of Pediatrics, Division of Hematology/Oncology, University of Texas Southwestern Medical Center, Dallas, Texas, USA | [2]Quantitative Biomedical Research Center, Department of Health Data Science and Biostatistics, Peter O'donnell, Jr., School of Public Health, University of Texas Southwestern Medical Center, Dallas, Texas, USA | [3]Department of Medicine, University of Chicago Pritzker School of Medicine, Chicago, Illinois, USA | [4]Division of Hematology/Oncology, Department of Pediatrics, University of Chicago Pritzker School of Medicine, Chicago, Illinois, USA | [5]Department of Pediatrics, Division of Hematology/Oncology, and Duke Cancer Institute, Duke University School of Medicine, Durham, North Carolina, USA | [6]Children's Oncology Group Statistics and Data Center, Department of Biostatistics, University of Florida, Gainesville, Florida, USA

Correspondence: Stephen X. Skapek (stephen.skapek@duke.edu)

Received: 25 November 2025 | **Revised:** 18 May 2026 | **Accepted:** 21 May 2026

Keywords: Bayes theorem | DNA copy number variations | Neuroblastoma | N-Myc proto-oncogene protein | oncogenes

ABSTRACT

Identifying targetable oncogenic drivers remains a challenge in neuroblastoma, the most common extracranial solid malignancy in children. We applied a Bayesian algorithm for integrative analysis of expression and copy-number, iExCN, to nominate oncogenic drivers in neuroblastoma. The iExCN algorithm found 47 oncogenes from a dataset of 195 neuroblastoma biopsy specimens. The nominated oncogenes included some previously implicated in neuroblastoma, including *ALK*, *MDM2*, *MYCN*, and *XPO1*, but most have not been linked to this disease. A CRISPR/Cas9-based screen testing those candidates revealed neuroblastoma cell line-specific and shared vulnerabilities in three well-characterized models, and dependencies were confirmed by complementary RNA knockdown. Analysis of more than 30 additional neuroblastoma cell lines using DepMap confirmed statistically significant dependency scores in the iExCN genes. Finally, analysis of two cohorts of children with neuroblastoma revealed a trend toward worse survival in cases in which more iExCN genes showed copy number gains. Our findings uncover multiple, potentially targetable oncogenic drivers that appear to influence neuroblastoma biology, demonstrating a generalizable capacity for iExCN to unmask disease genes and therapeutic targets in cancer.

1 | Introduction

Recently, new molecular genetic approaches and sophisticated bioinformatics tools have identified genetic mutations and illuminated the molecular basis of many cancer hallmarks [1], but only rarely has that insight reached the clinic in the form of novel therapy. This shortcoming is variably due to the paucity or the vast number of somatic single nucleotide variants (SNV) in an individual tumor, the limited recurrence of targetable SNVs across histologically similar tumors, an inability to target a mutant cancer-driving proteins, or the irrelevance of individual aberrations [2]. Large-scale approaches to "match" an individual patient's tumor to a molecularly targeted therapy have been conducted in adults and children, [3–5], but matches are only found

Abbreviations: CN(V), copy number [variant(s)]; FDR, false discovery rate; IPTG, isopropyl-beta-D-thiogalactopyranoside; NB, neuroblastoma; SCA, segmental chromosomal aberration(s); SNV, single nucleotide variant(s).

Previous Presentations: Advances in Neuroblastoma Research, Washington, DC. May 2025.

Lin Xu and Arhanti Sadanand are equivalent contributors to the manuscript.

Study Highlights

- What is the current knowledge on the topic?
  - iExCN is a recently developed analysis pipeline that has been successfully used to nominate cancer drivers in rhabdomyosarcoma. Neuroblastoma is an often-aggressive childhood cancer with prognostic biologic features including the amplification of the *MYCN* oncogene and the presence of segmental chromosomal aberrations. Since neuroblastoma is known to be a copy-number-driven disease similar to rhabdomyosarcoma, there is rationale for applying the iExCN algorithm to neuroblastoma to try to elucidate vulnerabilities to novel therapies.
- What question did this study address?
  - This study addressed whether a previously validated computational pipeline, iExCN, could identify novel therapeutic targets in neuroblastoma.
- What does this study add to our knowledge?
  - We found that applying the iExCN pipeline to neuroblastoma identified several targetable candidates that appeared to be expressed independently of *MYCN* within neuroblastoma. Target candidates were screened using knockdown methods to evaluate for effects on cell proliferation and cell line dependency. Two of the most promising candidates were *XPO1* and *SF3B1*, located on chromosomes 2p and 2q, respectively.
- How might this change clinical pharmacology or translational science?
  - Early-phase clinical trials have examined the use of *XPO1* inhibition and PARP inhibition in children with relapsed or refractory solid malignancies. While these studies included small numbers of patients with neuroblastoma, prior data support the continued investigation of these agents in specific patients with neuroblastoma. Additional studies may consider the investigation of these candidate therapies in combination with chemoimmunotherapy.

in a minority of cases, [5, 6], and treatment responses in adults have generally been poor [7].

The above challenges are prominent in neuroblastoma, the most common solid malignancy in children, even though much is known about the disease biology [8]. Amplification of *MYCN* has long been known to correlate with advanced-stage disease and poor survival in NB, [9] but the tumor harbors few somatic mutations, [10] such as activating mutations in *ALK* and inactivating mutations in chromatin remodeling genes *ATRX*, *ARID1A*, and *ARID1B* [11, 12]. *ALK* inhibitors are currently being evaluated as part of upfront therapy in the relatively few children with high-risk NB with ALK aberrations, but that represents only a minority of cases. Cytogenetic and molecular approaches have identified other clinically relevant segmental chromosomal aberrations (SCA), including gain of chromosome 17q and losses at chromosomes 1p and 11q [13, 14]. While these aberrations represent robust prognostic biomarkers, it is unknown how certain SCAs interact with other tumor biologic factors to affect outcomes. Due to the very large number of genes within each SCA, studies to date have not broadly assessed which of those many genes are likely to be true cancer drivers or suppressors [15]. Importantly, *MYCN* amplification is not sufficient to explain poor outcomes in those with the highest-risk disease, and that impedes efforts to identify targetable oncogenic drivers [13–16].

In mutation-poor cancers like NB, the malignant phenotype is likely determined by the expression of key cancer drivers and tumor suppressors, and copy-number gains and losses represent one way to govern expression levels. Bioinformatics analyses that integrate gene copy-number and expression levels have previously been utilized to uncover cancer drivers, and some are good but imperfect predictors of true oncogenic drivers [17]. To improve on this, we previously developed a new integrative analysis pipeline named iExCN that employs Bayesian logic to integrate gene expression changes correlating directionally with CNVs [18]. We applied the iExCN pipeline to matched expression and copy-number variant (CNV) datasets for rhabdomyosarcoma, a cancer that commonly affects children and adolescents. Similar to neuroblastoma, a minority of rhabdomyosarcoma cases harbor protein-altering mutations in certain oncogenes, but there are no highly recurrent and targetable mutations [19]. We used the iExCN pipeline to nominate 25 genes as oncogenes based on gene expression and copy number gains. Some of the cancer drivers identified this way were previously linked to rhabdomyosarcoma and, importantly, tumors with a greater number of iExCN genes displaying CN gains had worse outcomes [18]. Hence, we considered whether iExCN might also nominate oncogenic drivers that might have prognostic value in NB.

Here, we report on the initial use of iExCN in neuroblastoma to achieve three objectives: (1) to nominate oncogenic drivers in NB; (2) to provide functional validation of iExCN-nominated oncogenes using a CRISPR/Cas9 mini-pool and other functional genomics approaches across a panel of over 30 NB cell lines; and (3) to explore the value of CN changes in iExCN-defined genes as a molecular prognostic biomarker for children with this disease.

2 | Methods

2.1 | Neuroblastoma Genomic Datasets

Matched CN and gene-expression data were from two separate NB patient cohorts: (1) 195 NB patients in the "GMKF-NB" cohort (dbGaP phs001228), and (2) 344 NB patients from the "TARGET-NB" cohort (dbGaP: phs000218). Information about requesting these and similar datasets can be found at the NIH Database of Genotypes and Phenotypes (https://dbgap.ncbi.nlm.nih.gov/home/). Patients from GMKF-NB and TARGET-NB were linked to the International Neuroblastoma Research Group data commons (INRGdc) through Universal Specimen Identifiers [20]. Patient data were retrieved as described previously [21]. The INRGdc and data use are approved by the

University of Chicago institutional review board, which waived consent as all data were de-identified.

2.2 | DNA Sequence, Gene CN, and Gene Expression Analyses

Whole-genome reads were aligned to hg38. Significantly altered CNVs were examined by the Genomic Identification of Significant Targets in Cancer (GISTIC) method using a default q-value of 0.25 to define statistical significance, as previously described [22]. For gene expression data analysis, raw RNA sequencing reads underwent adapter removal and quality-filtering using Cutadapt [23]. Alignment to hg38 was performed with HISAT2 [24]. Differential gene expression analysis was conducted by DESeq2 [25]. Pathway enrichment analysis using pathway sets from the Molecular Signatures Database (MSigDB) identified significantly enriched pathways based on an FDR-adjusted p-value < 0.05.

2.3 | iExCN Analysis Pipeline

In brief, the iExCN analysis pipeline employs Bayesian statistics to calculate the likelihood that gene expression is driven by gene CN [18–27]. Three steps in the pipeline are: (1) convert input (paired CN and expression data) to the matrix format for Bayesian estimation, (2) use *Markov chain Monte Carlo* to estimate posterior probability of group differences in gene expression, and (3) summarize the statistical results (Figure 1A). The probability that group difference is greater than zero must be more than 99.9% in Bayesian estimation, as previously established [26–28]. To minimize false-positive candidates, we applied a deep learning model that processed and analyzed over one million PubMed publications, generating a comprehensive list of cancer-related genes (L. Xu, in preparation) as the focus of the iExCN analysis. A detailed description of the computational steps is provided in Figure S1. The iExCN scripts are licensed under the GNU General Public License v3.0, and we make them available at https://github.com/Lin-Xu-lab/iExCN.

2.4 | Cell Culture Models

NB cell lines (Kelly, SK-N-AS, and SHEP) were grown at 37°C with 5% CO_2 in RPMI 1640 (Gibco, 11875–093) supplemented with 10% heat-inactivated FBS (Gibco, 26140–079), 2 mmol/L l-glutamine (Gibco, 25030–081), and 1% Antibiotic-Antimycotic (Gibco, 15240–062). Kelly cells were obtained from ATCC, SK-N-AS were a kind gift from Dr. John Maris, and SHEP cells were a kind gift from Dr. June Biedler. NB cells were authenticated by short tandem repeat (STR) testing and confirmed to be mycoplasma-free.

2.5 | CRISPR/Cas9 "Mini-Pool" Screen and Data Analysis

Kelly, SK-N-AS, and SHEP cells were transduced with the library cloned in lentiCRISPRv2 lentiviral vector and analyzed as previously described [18–29]. Lentiviral vectors included sgRNA guides targeting positive controls (genes established to be essential in mammalian cells) [18–30], negative controls (randomly selected from all genes expressed in neuroblastoma specimens), and iExCN-predicted oncogenes were designed as described (Table S1) [31]. Three iExCN-predicted genes were excluded as they had four or more sgRNAs with high "off-target" scores: *H3F3B*, *RGPD3*, and *SRSF2*. Following transduction at an MOI of 0.3, cells were cultivated in 5 μg/mL puromycin through ~20 population doublings before harvesting genomic DNA. Each cell line had a biological replicate that was transduced, cultivated, and processed in parallel.

Genomic DNA, harvested from two replicates each on day 0 and passage 20, was sequenced using an Illumina NovaSeq 6000. The supporting reads, normalized to reads from non-targeting controls, were trimmed using cutadapt v4.1 [23], and MAGeCK v0.5.9.5 [32] was used to collect gene-level sgRNA read counts and rank sgRNAs. p values for fold change comparisons of gene-level read counts between day 0 and passage 20 were adjusted using FDR. An adjusted $p < 0.05$ was considered significant.

2.6 | DepMap CRISPR/Cas9 Gene Dependency Analysis

Dependency scores for 44 of the iExCN genes, along with positive and negative controls, were determined from the Broad Institute Cancer Dependency Map and analyzed in R using the DepMap and ExperimentHub packages available through Bioconductor [33]. *FAT3*, *RGPD3*, and *H3F3A* did not have data available in the 22Q2 release. Gene dependency probabilities were determined across the 34 NB cell lines, including Kelly and SK-N-AS, used in our own studies, and SK-N-SH, from which SHEP cells were derived.

2.7 | Protein and RNA Expression

Western blotting of NB cell line lysates was performed as previously described [34], with primary antibodies directed against XPO1 (#46249; Cell Signaling), SF3B1 (#14434; Cell Signaling), and GAPDH (#47724; Santa Cruz). RNA expression was quantified by real-time RT-PCR with the RNeasy Mini Kit (Qiagen), 1×Power SYBR Green Master Mix (Applied Biosystems), and IDT PrimeTime Primers (Table S2), essentially as previously described [18]. The data shown represent at least two independent experiments.

2.8 | Gene Knockdown and Cell Accumulation

siRNA-mediated knockdown experiments were carried out as previously described [18]. The siRNA duplexes targeting desired genes were predesigned and purchased from Sigma; the ID number of predesigned siRNA for each gene of interest is listed (Table S2). Cells were harvested at either 48 h after the initial transfection for RT-qPCR or six days for the cell proliferation assay. Cell accumulation was assayed using the CyQUANT Cell Proliferation Assay Kit (Invitrogen) according to the manufacturer's instructions. Sample fluorescence was measured using a CLARIOstar Microplate Reader (BMG Labtech).

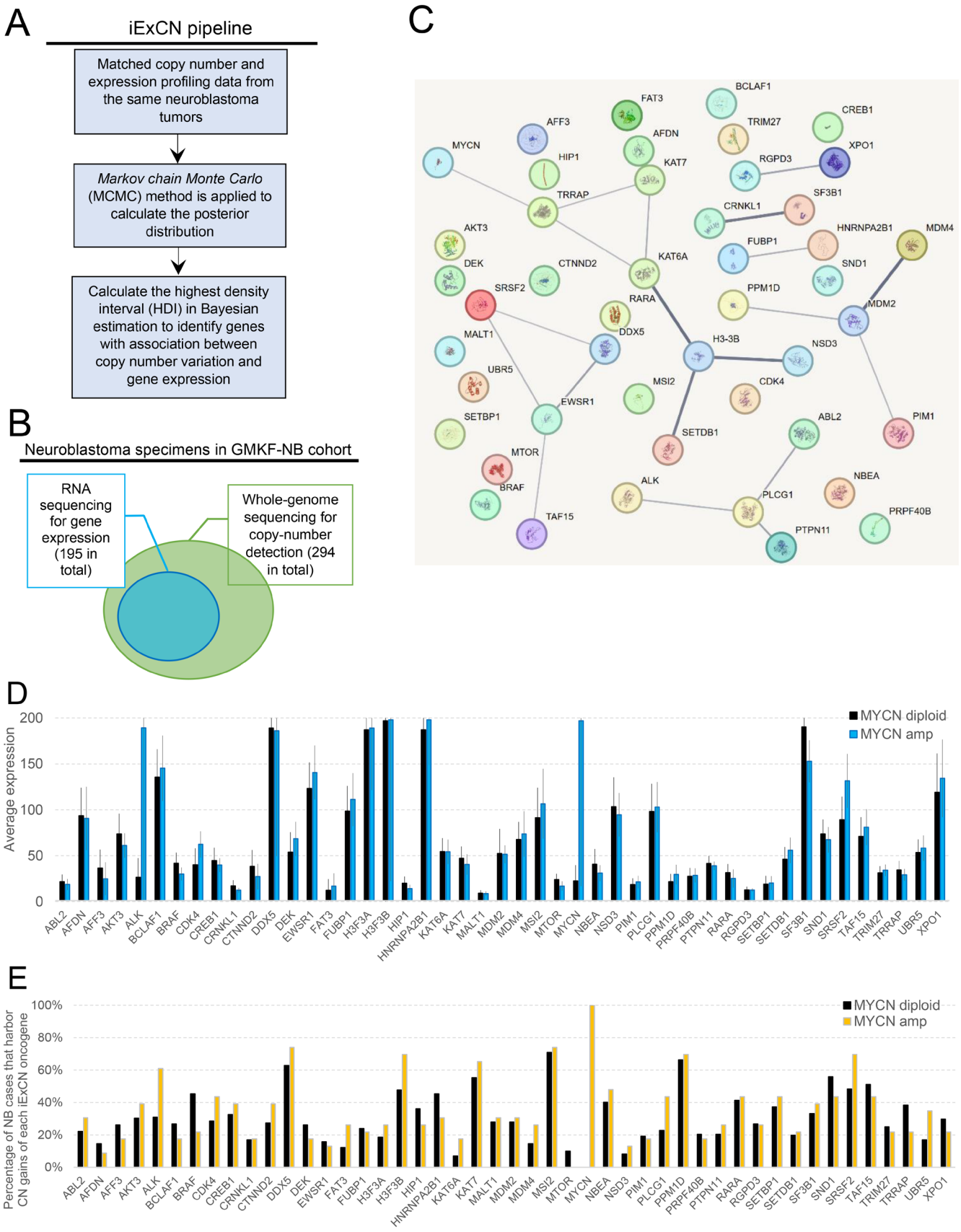

FIGURE 1 | Legend on next page.

FIGURE 1 | The iExCN analysis identifies candidate oncogenic drivers in neuroblastoma (A) Steps in the iExCN analysis pipeline. (B) The number of cases with whole-genome and RNA sequencing from the same biopsies used in the primary analysis of the GMKF-NB cohort. (C) Schematic depiction of iExCN nominated oncogenes with protein–protein interactions network from the Search Tool for the Retrieval of Interacting Genes/Proteins (STRING) database. (D) Average expression level of iExCN-identified oncogenes in NB specimens with diploid and amplified *MYCN*, as indicated, in the GMKF dataset. Gene expression units: Fragments Per Kilobase of transcript per million mapped reads (FPKM). (E) The frequency of CN gains among iExCN-nominated oncogenes across the GMKF-NB dataset.

2.9 | Statistical Analysis

Statistical analyses were conducted using R programming packages (http://www.R-project.org). The comparison of two independent samples was assessed using the two-tailed Student's *t*-test (normal distribution) or nonparametric two-tailed Mann–Whitney *U* test (non-normal distribution). p values <0.05 were considered statistically significant. Kaplan–Meier plots were generated, with differences between high- and low-expression groups assessed using the log-rank test. p values <0.05 were considered statistically significant.

3 | Results

3.1 | Using iExCN to Nominate Oncogenic Drivers in Neuroblastoma

CNVs are well-described in NB, and *MYCN* amplification has long been recognized to correlate with poor outcome [35, 36]. The discovery cohort of 195 NB patients from the GMKF-NB dataset included both RNA-seq data for gene expression and whole-genome sequencing data for CN alterations (Table 1). *MYCN*-amplified tumors had no significant difference in the percentage of genes with CN gains and losses across the genome on average than cases without *MYCN* amplification (Mann–Whitney test, $p>0.05$) (Figure S2).

Given the large number of CNVs in NB, we filtered the genes in which copy-number gain was not associated with increased expression using the iExCN pipeline (Figure 1A). Applying iExCN to the discovery cohort returned a list of 47 candidate oncogenes, displayed with known human protein–protein interactions based on the STRING database (Figures 1B,C, and Table S3). With the notable exception of ALK, expression of the nominated oncogenes did not substantially vary based on *MYCN* status (Figure 1D). Recurrent CN gains of iExCN-predicted oncogenes across the entire dataset were also high in cases with and without *MYCN amplification*, a notable exception is *MTOR*, gains of which were noted only in *MYCN-diploid* cases (Figure 1E).

Pathway analysis using the MSigDB database revealed that the 47 genes represented 22 different biological pathways (Table S4), including (1) *RNA Polymerase II Transcription* (q value $=8.0\times10^{-9}$, 16 genes: *AKT3*, *CDK4*, *CREB1*, *DEK*, *H3-3A* and *H3-3B*, *KAT6A*, *MDM2*, *MDM4*, *MTOR, RARA*, *PPM1D*, *PTPN11, SRSF2*, *TAF15*, and *XPO1*); (2) signal transduction by growth factor receptors and second messengers (q value $=1.3\times10^{-8}$, 11 genes: *AKT3*, *ALK*, *BRAF*, *CREB1*, *HIP1*, *MDM2*, *MTOR*, *PIM1*, *PLCG1*, *PTPN11*, and *SND1*); and (3) ErbB signaling (q value $=1.5\times10^{-6}$, 6 genes: *ABL2, AKT3*, *BRAF*, *MDM2*, *MTOR*, and *PLCG1*).

3.2 | Candidate iExCN Oncogenes Inform Our Understanding of Clinically Relevant Segmental Chromosome Gains

Beyond *MYCN* amplification, other segmental chromosomal gains including 1q, 2p, 12q, and 17q are commonly accepted to confer poor prognosis in patients with NB [9–37]. Clinical risk stratification tools typically consider tiers of low-, intermediate-, and high-risk NB [37]. The number of iExCN genes harboring CN gains increased in an essentially linear fashion within each clinical risk group, and approximately 10% of cases harbored no gains in iExCN genes (Figure S3A). With the exception of *MYCN*, CN gains were of low-amplitude (Figure S3B), similar to rhabdomyosarcoma [18]. The number of cases harboring CNVs in an individual iExCN gene increased from *MTOR* and *KAT6A*, found in fewer than 20 cases, to *DDX5*, *MSI2*, and *PPM1D*, each found in more than half of the cases in the dataset (Figure S3C). The distribution of individual iExCN gene gains did not correlate with clinical risk group (*t*-test, $p>0.05$ for any two comparisons).

Twenty of the 47 candidate oncogenes nominated by iExCN resided within the regions of chromosomes 1q, 2p, 12q, and 17q, for which copy-number gains are associated with poorer survival (Table S5). When considering all genes located at two of these, we found that incorporating a rigorous Bayesian probability score ($\geq$99.9%) dramatically limited the number of candidates (Figure 2A, Y-axes). Thirteen of the 47 oncogenes nominated by iExCN lie within these two segments: five on 1q and eight on 17q.

Because copy-number gains in iExCN genes *cooperatively* influenced rhabdomyosarcoma outcomes [18], we explored the co-occurrence of iExCN CN gains in NB. When considering all possible pairs, and assuming independent assortment, we found 626 pairs with a probability of 1 that expected co-occurrence frequency would be less than the observed (Table S6). Thirteen gene pairs displayed a co-occurrence rate four or more times greater than expected (Figure 2B), with the greatest enrichment of *KAT6A* and *NSD3*, both localized to chromosome 8p. Twelve of those pairs were located on the same chromosome, and six were on the same chromosomal arm, including chromosome 1q four times (Figure 2C). The single outlier was *PRPF40B* and *MTOR* on chromosomes 12q and 1p, respectively.

We also explored the status of iExCN candidates localized to chromosomes 1q, 2p, and 17q, which are frequently gained in NB. Approximately 25% of the cases had no CN gains in any of the candidate genes found on those chromosomal segments. In cases harboring gains in any gene on one of these segments, approximately 40%–50% of the cases harbored gains in all the candidates on that segment (Figure 2D). Taken together, these data

TABLE 1 | Clinical and demographic features of the analyzed cohorts.

Feature	Discovery cohort (GMKF, $n = 195$)	Clinical validation (TARGET, $n = 344$)
Age, months median (Q1- Q3)	13 (5–29)	22 (7–42)
Sex, no. (%)		
Male	97 (49.7%)	185 (53.8%)
Female	98 (50.3%)	159 (46.2%)
Race, no. (%)		
White	165 (84.7%)	274 (79.7%)
Black	11 (5.6%)	36 (10.5%)
Asian	7 (3.6%)	7 (2.0%)
American indian/Alaskan native	1 (0.5%)	1 (0.3%)
Native hawaiian/Pacific islander	0 (0%)	1 (0.3%)
Unknown	11 (5.6%)	25 (7.2%)
Ethnicity, no. (%)		
Non-Hispanic	180 (92.3%)	305 (88.7%)
Hispanic	8 (4.1%)	20 (5.8%)
Unknown	7 (3.6%)	19 (5.5%)
INSS stage, no. (%)		
1	55 (28.3%)	55 (16.0%)
2	40 (20.5%)	41 (11.9%)
3	27 (13.8%)	35 (10.2%)
4S	19 (9.7%)	38 (11.0%)
4	54 (27.7%)	174 (50.6%)
Unknown	0 (0%)	1 (0.3%)
INPC Grade, no. (%)		
Undifferentiated/Poorly differentiated	166 (85.1%)	284 (82.6%)
Differentiating	20 (10.3%)	29 (8.4%)
Unknown	9 (4.6%)	31 (9.0%)
MYCN Status, no. (%)		
Amplified	22 (11.3%)	53 (15.4%)
Not amplified	172 (88.2%)	288 (83.7%)
Unknown	1 (0.5%)	3 (0.9%)
Primary tumor site, no. (%)		
Adrenal	69 (35.4%)	134 (39.0%)
Abdominal/retroperitoneal	61 (31.3%)	123 (35.8%)
Neck	12 (6.2%)	14 (4.1%)
Thorax	31 (15.9%)	40 (11.6%)
Pelvis	12 (6.1%)	17 (4.9%)
Other	7 (3.6%)	8 (2.3%)
Unknown	3 (1.5%)	8 (2.3%)

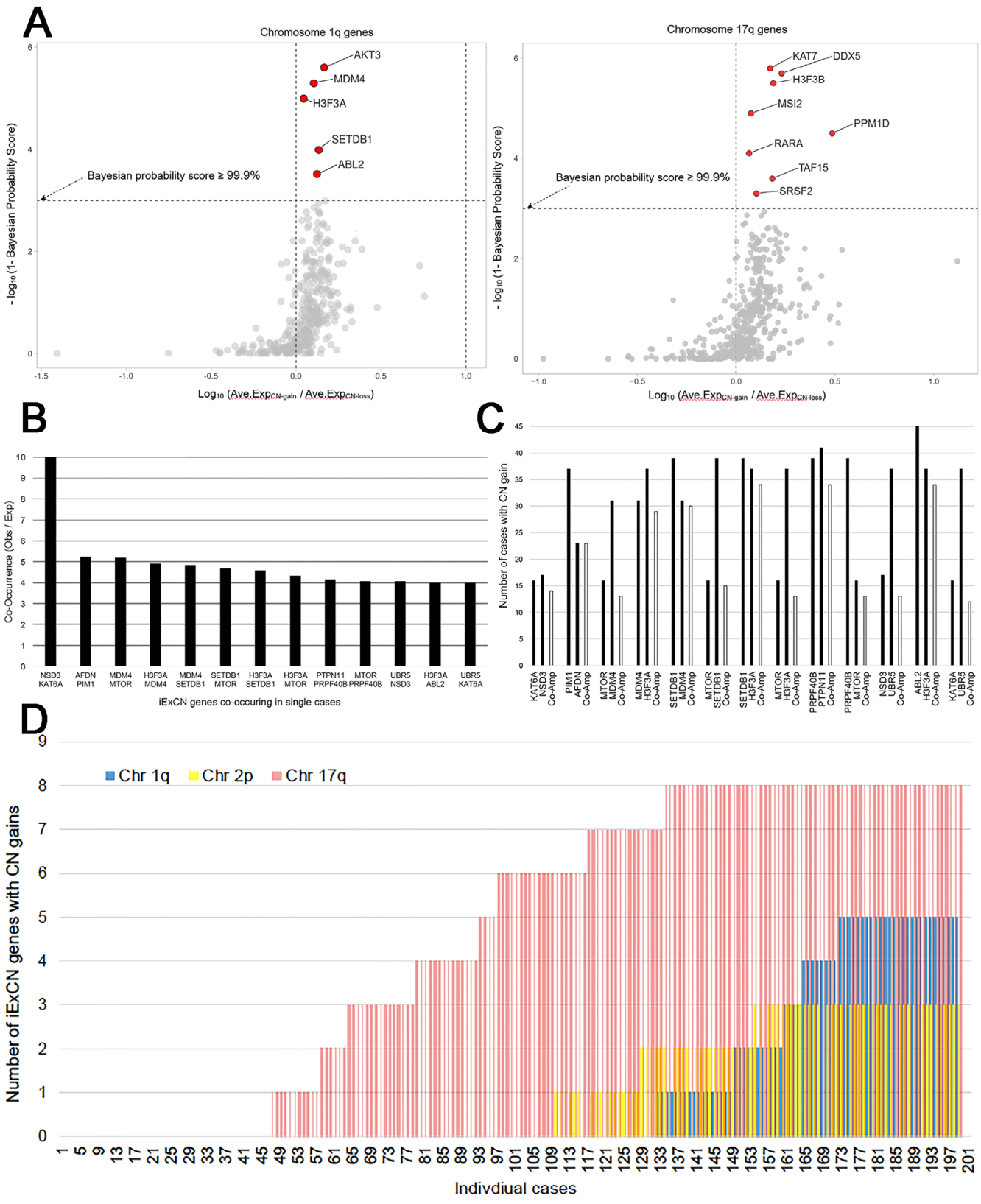

FIGURE 2 | Co-amplification patterns in iExCN-nominated oncogenes found within chromosomal arms commonly amplified in neuroblastoma (A) iExCN pipeline identifies candidate oncogenes among hundreds of genes on chromosome 1q and 17q, frequently amplified in neuroblastoma. (B and C) The 13 iExCN gene pairs in which the frequency of co-amplification was significantly enriched at least 4-fold more than the frequency based on chance (D) The frequency of co-amplification of the 3, 5, and 8 iExCN candidates residing at chromosomes 2p, 1q, and 17q, respectively.

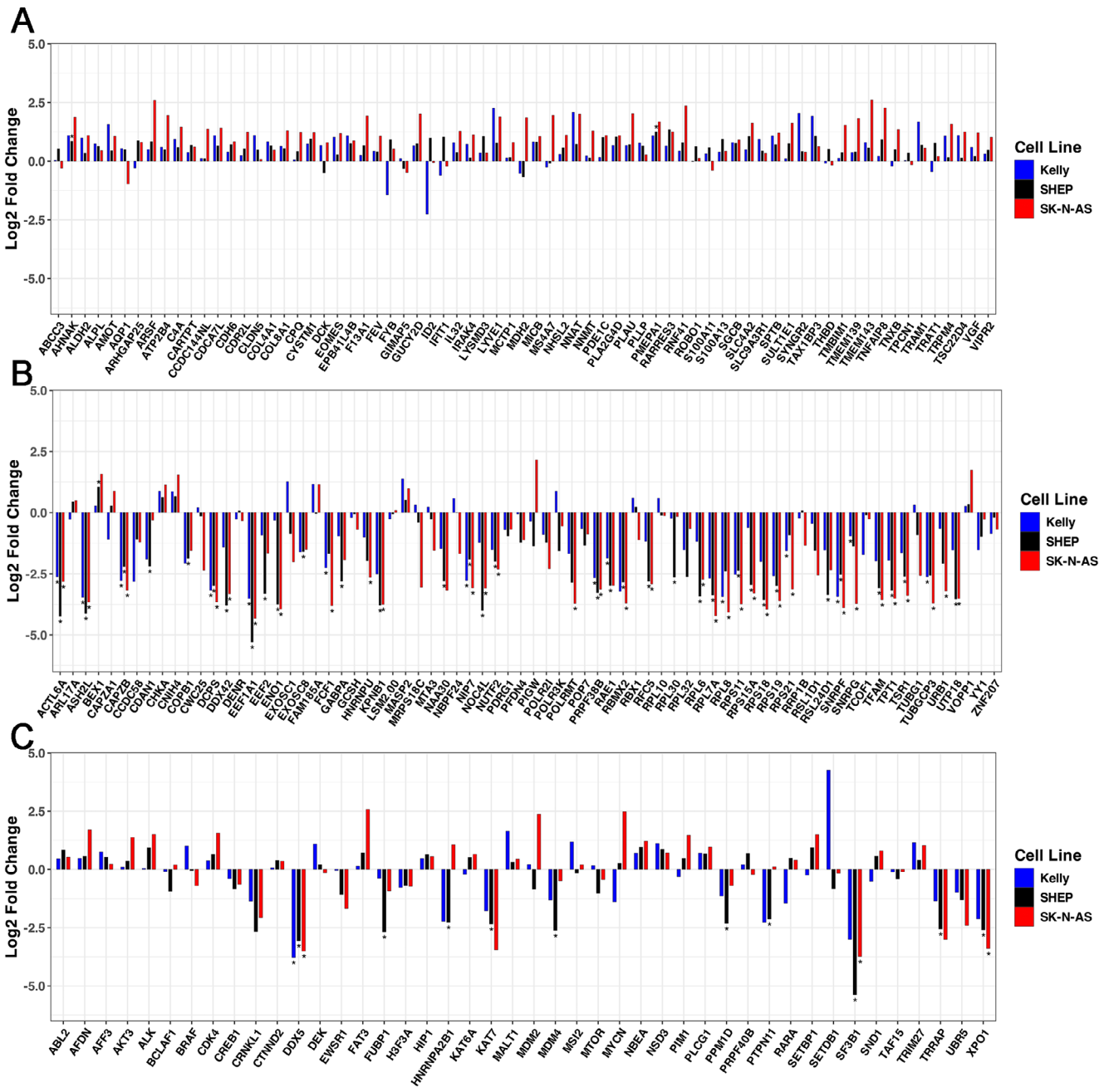

FIGURE 3 | Depletion of iExCN-nominated oncogenes in a CRISPR/Cas9 mini-pool screen (A, B, and C): Relative fold change in the representation of sgRNA guides targeting the indicated genes as negative controls (A), positive controls (B), and iExCN candidates (C) in the indicated cell lines. Asterisks (*) in B and C signify the changes that are statistically significant.

point toward the oncogenes that may—individually or cooperatively—be contributing to poorer outcomes driven by gains in 1q, 2p, and 17q.

3.3 | Functional Validation of iExCN Candidates in Neuroblastoma Cell Lines

We functionally validated the iExCN genes using a CRISPR/Cas9 "mini-pool" targeting candidate oncogenes in an essentiality screen using well-characterized NB models. We found that only two of 71 vectors targeting negative controls were significantly enriched, and none were depleted (Figure 3A). In contrast, 42 of 74 vectors targeting genes known to be essential were depleted in one or more of the tested NB lines, confirming the expected assay performance (Figure 3B). For iExCN-defined genes, ten of 44 vectors targeting candidate oncogenic drivers were significantly depleted in one or more cell lines (Figure 3C), indicating that these oncogenes were required for in vitro propagation in the tested models.

We compared the data from our drop-out screen to dependency scores in DepMap. Gene dependency scores for iExCN genes, negative controls, and positive (essential) controls were also analyzed in Kelly, SK-N-AS, and SK-N-SH cell lines for comparison to the CRISPR/Cas9 mini-pool screen. Guides targeting

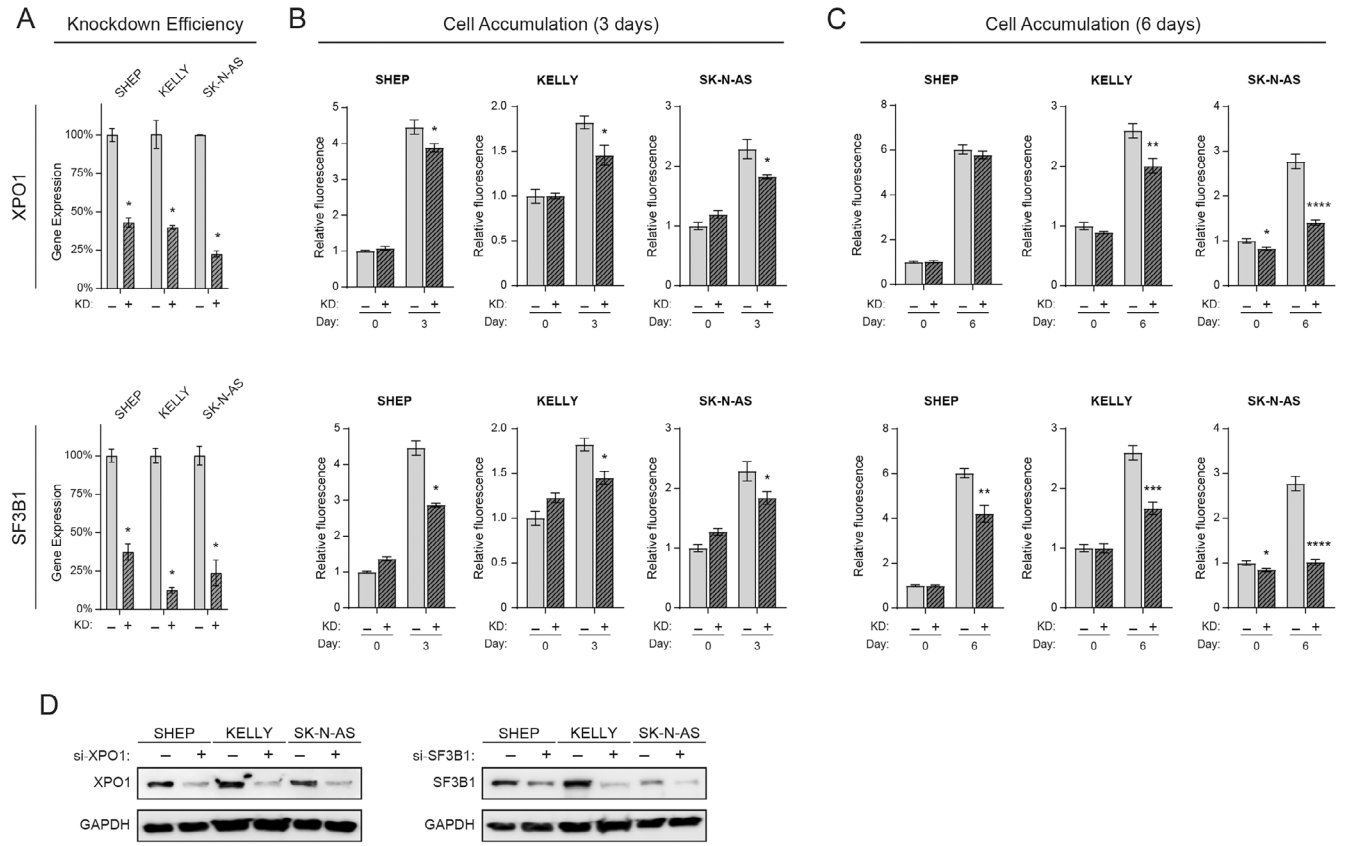

FIGURE 4 | Knockdown of XPO1 and SF3B1 siRNA reduces cellular accumulation in three neuroblastoma cell lines (A and D) The effect of XPO1 and SF3B1 knockdown, following targeted siRNA treatment for 48 h, was determined by (A) mRNA expression through qRT-PCR and (D) protein levels through Western blot. (B and C) The effect of XPO1 and SF3B1 knockdown on cell accumulation in SHEP, Kelly, and SK-N-AS cell lines was assessed by CyQuant assay after a (B) 3-day or (C) 6-day incubation following initial siRNA treatment. Graphs are of a single experiment with six biological replicates per group. **** = $p < 0.0001$, *** = $p < 0.001$, ** = $p < 0.01$, measured by two-tailed unpaired *t*-test.

10 genes were significantly depleted in mini-pool analysis in SHEP, and seven of those had negative mean dependency scores in SK-N-SH, from which SHEP cells were derived. All four of the genes with significantly depleted guides in our SK-N-AS and Kelly CRISPR/Cas9 screen also had negative dependency scores in DepMap (Figure S4).

Based on these results, we further validated nine of the genes using transient siRNA knockdown (Figure 4 and Figure S5). Apart from *MDM4* and *PPM1D*, knocking down each gene reduced cell accumulation in one or more of the tested lines, and the effects were generally greater at 6 days. This finding confirmed that their drop-out in the CRISPR/Cas9 screen was not due to a Cas9-imposed DNA damage response that can occur in such a screen [38].

3.4 | The Majority of Individual iExCN Genes Are Dependencies in Neuroblastoma Cell Lines

We leveraged DepMap to further assess the importance of these iExCN genes in 34 neuroblastoma cell lines in that dataset. The mean gene dependency scores were determined for each gene across the 34 available cell lines and visualized by boxplot. Thirty-four of 44 (77%) iExCN genes had mean dependency scores less than zero with a mean dependency score of all iExCN genes found to be −0.438 (Figure 5A, and Figure S6). This significantly differed from the randomly chosen, negative control genes used in our CRISPR/Cas9 screen, for which the mean dependency scores clustered around 0 (Figures S6 and S7). Of note, the mean dependency score for iExCN genes was significantly more negative than the randomly chosen negative controls ($p < 2 \times 10^{-16}$; ANOVA with Tukey post hoc test), further highlighting the capacity for iExCN to define vulnerabilities.

Mean gene dependency probabilities of iExCN genes were also calculated per NB cell line and visualized by boxplots (Figure 5B). Nine genes had negative dependency scores outside of the boxplot boundaries. These so-called outliers were distributed across the tested cell lines with an average of 3.5 ± 0.29 in each cell line. Five of those (*CRNKL*, *SF3B1*, *SRSF2*, *TRRAP*, and *XPO1*) were outliers in at least 19 of 34 cell lines (Figure 5C). Seven of these (*CRNKL1*, *DDX5*, *MTOR*, *SF3B1*, *SRSF2*, *TRRAP*, *XPO1*) are characterized as common essential genes by DepMap; those that are not among common essential genes may be particularly interesting as potential therapeutic targets for neuroblastoma.

3.5 | Number of iExCN Genes With CNV Gain as a Potential Prognostic Biomarker

We examined whether the number of iExCN oncogenes harboring CNVs influenced outcomes in children with high-risk

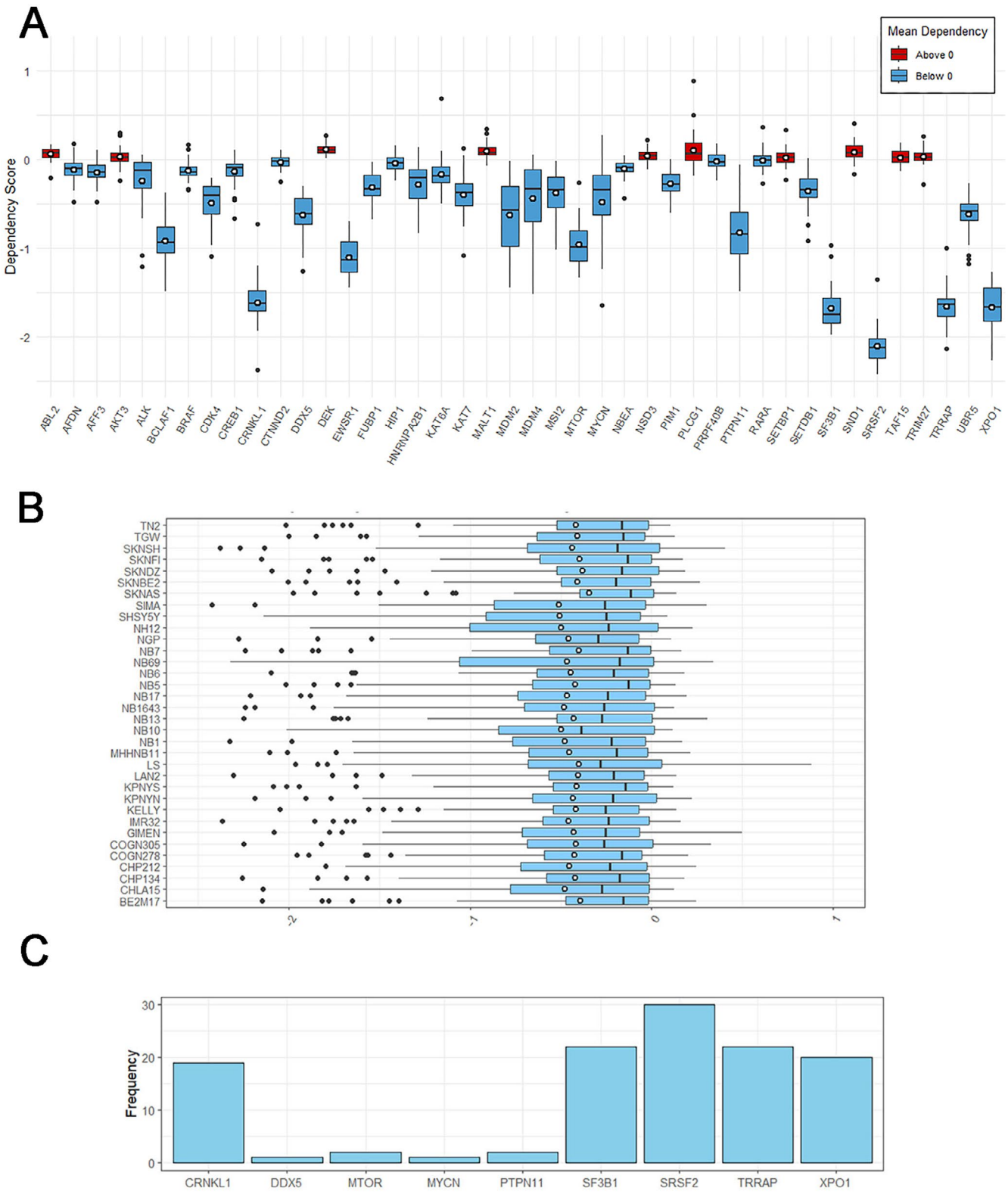

FIGURE 5 | DepMap shows that most iExCN-defined genes have negative dependency scores across a panel of 34 neuroblastoma cell lines (A) Mean DepMap dependency scores of iExCN genes across 34 neuroblastoma cell lines. (B) Mean DepMap gene dependency scores of iExCN genes in each neuroblastoma cell line. (C) The number of neuroblastoma lines in which specific "outlier" genes have dependency scores that fall outside of the boxplot boundaries.

NB. Using two separate cohorts of high-risk patients, we found that cases with 25 or fewer iExCN genes containing CN gain displayed a trend toward better overall survival than those with more than 25 iExCN genes involved, although it did not reach significance (log-rank test; $p = 0.08$ for the GMKF cohort and $p = 0.069$ for the TARGET cohort) (Figure 6A).

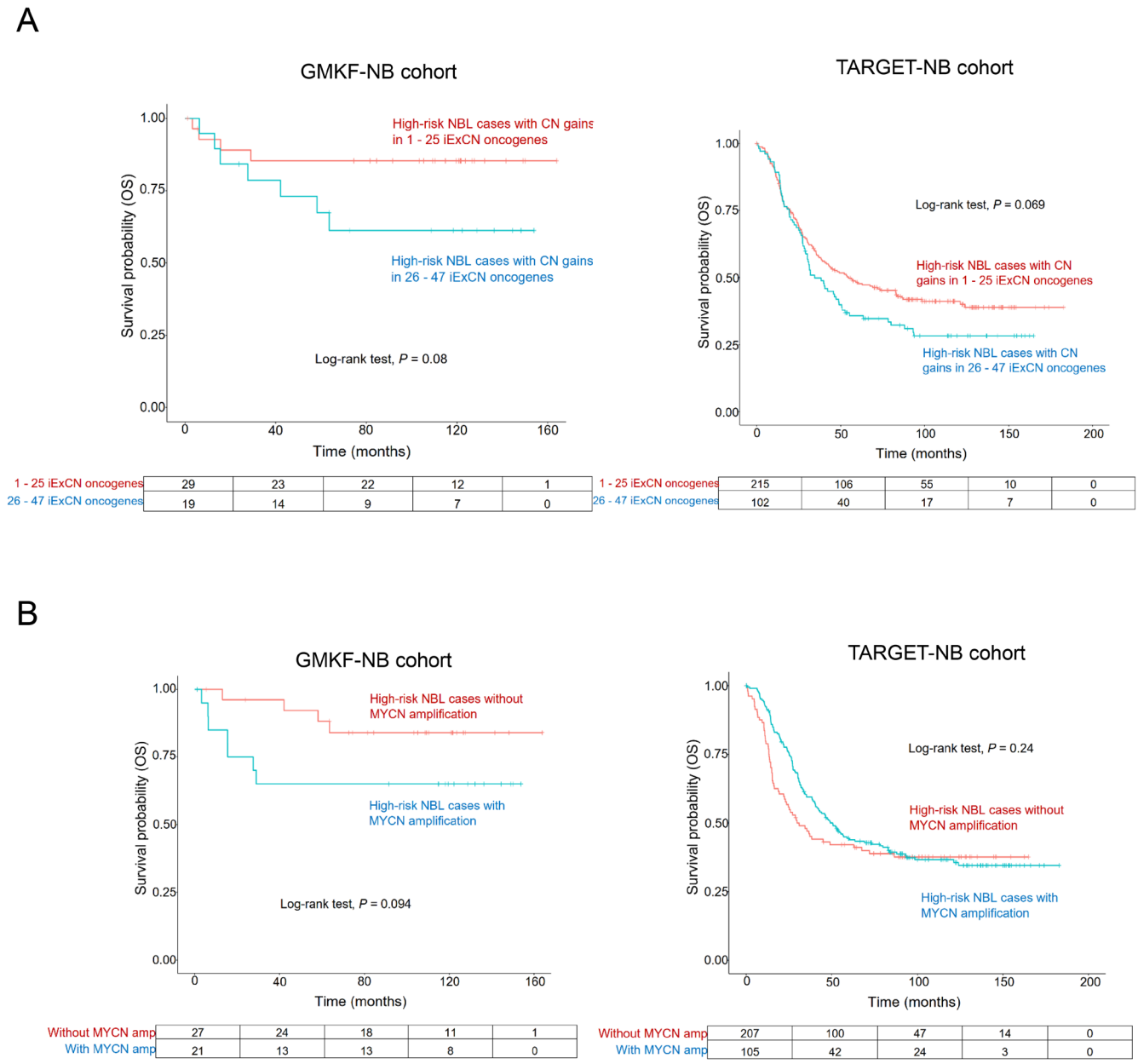

FIGURE 6 | There is a non-significant trend toward poorer survival in neuroblastoma in which more than 25 iExCN genes demonstrate CN gain (A) Kaplan–Meier plots display overall survival in two independent cohorts with different numbers of iExCN genes with CNVs, as indicated. (B) Kaplan–Meier plots display overall survival in two independent cohorts with or without *MYCN*-amplification.

Because *MYCN* amplification is a well-established prognostic factor in this disease—and *MYCN* was among our iExCN genes—we assessed whether the survival trends were merely driven by *MYCN*. We note that the fraction of cases with and without *MYCN* amplification was the same in cases with iExCN gains in 25 or less versus more than 25 iExCN genes in each cohort (Fisher exact, 2-tailed, p value: 0.309 and 0.576 in the TARGET and GMKF datasets, respectively) (Table S7). In our two datasets of children with high-risk disease, *MYCN* amplification itself did (GMKF; $n = 48$) and did not (TARGET; $n = 312$) correlate with outcome (Figure 6B). Hence, how much iExCN genes add to *MYCN* for neuroblastoma risk stratification is not clear and merits further prospective testing.

4 | Discussion

The iExCN pipeline identified 47 candidate oncogenes in NB. Twenty of these were located on chromosome regions known to be associated with high-risk disease. There was no indication that iExCN nominated different oncogenes in *MYCN*-amplified or non-amplified tumors. Ten of our oncogenes were functionally validated as being crucial to propagation in a CRISPR screen using three distinct NB cell lines. The hit rate of 19% is comparable to that of other reported focused CRISPR screens and our previous rhabdomyosarcoma analysis [18–39]. Most of those 10 were further validated by siRNA in tested cell lines, which indicates that their identification in the CRISPR screen was not

merely due to Cas9-mediated DNA damage response. We also leveraged DepMap to explore candidates across more than 30 neuroblastoma lines. Beyond confirming the importance of five of our enriched genes in more than half of those lines, DepMap displayed line-to-line heterogeneity because four genes showed very strong dependency in only one or two of the cell lines. This heterogeneity is also evidenced by the fact that neither *ALK* nor *MYCN* were identified in our mini-pool screen. How the various dependencies correlate with neuroblastoma subtype is not yet clear. Finally, we tested the potential for the number of iExCN harboring copy-number gains to hold prognostic value. While there was a trend toward that goal in two datasets, it did not reach statistical significance. Taken together, these findings highlight the potential for the iExCN algorithm to nominate NB drivers based on integrating gene expression and CN gains, and the potential for those changes to be used in risk stratification.

With the exception of *ALK* and *MYCN*, we note that all the other genes nominated by iExCN had low-amplitude copy-number gains, a well-recognized feature of neuroblastoma [40] discussed further below. Interestingly, that finding is consistent with our previous report using iExCN to nominate oncogenes in rhabdomyosarcoma [18]. In rhabdomyosarcoma, more iExCN genes bearing copy-number gains significantly correlated with worse survival, implying a cooperative effect on rhabdomyosarcoma biology. Whether the same is true in neuroblastoma remains to be proven.

CNVs, particularly SCAs, are well described in high-risk NB, [41] and SCAs have established prognostic value [35–43]. Despite this long-standing knowledge, efforts to understand how these recurrent gains and losses affect individual oncogenes have led to a paucity of confirmed tumor-promoting drivers, with *CHD5* on chromosome 1p being the only tumor suppressor known to be consistently lost [44] and *MYCN* and *ALK* the only known oncogenes consistently gained by CNVs [45, 46]. That iExCN nominated additional genes at certain of those SCAs suggests their particular roles as drivers of the poorer outcomes. High expression of the candidates, regardless of *MYCN* status, suggests they are independent contributors to tumor biology. We found further evidence that some of these genes may work alone or cooperatively to influence tumor biology, based on a non-significant tendency toward worse survival in cases harboring gains in a greater number of iExCN genes. As coordinated transcriptional networks are established drivers of NB phenotype [47, 48], the potential for cooperative interactions of iExCN genes lying in proximity within an individual SCA will require experimental validation.

Two potentially targetable candidates that showed significance in nearly all methods and cell lines tested were *SF3B1* and *XPO1*. Both are located on chromosomal arms commonly altered in neuroblastoma (2q33.1 and 2p15, respectively) [49] and may be relevant for therapeutics. SF3B1 encodes a portion of the spliceosome, a complex responsible for the removal of introns from mRNA. Variants in SF3B1 have been identified as driving mutations behind myelodysplastic syndrome and other hematologic malignancies; SF3B1 mutations have also been identified in solid tumors including melanoma and neuroblastoma [50, 51]. A splicing modulator, pladienolide B, inhibited the growth of *MYC*-mutated small cell lung cancers in vitro [52], and a small molecule inhibitor H3B-8800 has been studied in patients with hematologic malignancies [53]. Data suggest that SF3B1 mutations may confer increased sensitivity to PARP inhibition [54], which has been shown to be safe and tolerable in pediatric patients with relapsed or refractory neuroblastoma [55]. *XPO1* encodes exportin-1 which transports proteins and RNA from the nucleus to the cytoplasm of cells. Located over 45 million base pairs from *MYCN* on chromosome 2p, and thus independent of the *MYCN*-amplificon [56], *XPO1* expression has been associated with poor prognosis in NB independent of age and stage. XPO1 inhibition using verdinexor, an alternative selective inhibitor of nuclear export, led to NB regression in both cell lines and xenograft models [57, 58]. Although no single agent responses were seen with selinexor in a phase 1 trial for children with relapsed/refractory solid tumors and central nervous system malignancies, the study included only two patients with NB [59]. With the potential for clinical assays to detect low-amplitude copy-number gains and gene expression in routine pathology specimens, it will be important to prospectively evaluate whether CN gains or high expression of *SF3B1* and *XPO1* can serve as molecular biomarkers predicting response to those inhibitors.

In summary, the iExCN pipeline is a validated bioinformatics tool that identified potentially targetable vulnerabilities in NB in a *MYCN*-independent manner. Functional validation using a CRISPR/Cas9 mini-pool supports two of our nominated oncogenes, *SF3B1* and *XPO1*, as potential targets. Additional functional evaluation of other iExCN candidates, evaluation of CN gains and expression as predictive biomarkers, and further deployment of iExCN in additional datasets are warranted.

Author Contributions

Lin Xu, Arhanti Sadanand, Yen-Ting Liu, Erin Butler, Flannery Bowman, Mark A. Applebaum, and Stephen X. Skapek wrote the manuscript. Lin Xu, Arhanti Sadanand, Erin Butler, Susan L. Cohn, Mark A. Applebaum, and Stephen X. Skapek designed the research. Lin Xu, Evan W. Neczypor, Yen-Ting Liu, Erin Butler, Kelley Moore, Flannery Bowman, Yamin Mazumder, Arlene Naranjo, and Alexandre Chlenski performed the research. Lin Xu, Flannery Bowman, Xue Xiao, Lei Guo, and Mark A. Applebaum analyzed the data.

Acknowledgments

The authors acknowledge Shireen Toubbeh for excellent technical assistance; the UT Southwestern Quantitative Biomedical Research Center and Bioinformatics Core of the Harold C. Simmons Comprehensive Cancer Center, funded by the NIH/National Cancer Institute (NCI) P30CA142543; the University of Chicago High Performance Computing Cluster and Sequencing Cores, funded by the NIH/NCI P30CA014599. The INRG Data Commons is supported in part by the St. Baldrick's Foundation, the Little Heroes Cancer Research Fund, Children's Neuroblastoma Cancer Foundation, Neuroblastoma Children's Cancer Foundation, the Super Jake Foundation, the Alex's Lemonade Stand Foundation, and The Matthew Bittker Foundation. Data included in the INRG database were provided by Children's Oncology Group (COG), Pediatric Oncology Group (POG), Children's Cancer Study Group (CCSG), German Gesellschaft für Pädiatrische Onkologie und Hämatologie (GPOH), European Neuroblastoma Study Group (ENSG), International Society of Pediatric Oncology Europe Neuroblastoma Group (SIOPEN), Japanese Neuroblastoma Study Group (JNBSG), Japanese Infantile Neuroblastoma Co-operative Study Group (JINCS), Spanish Neuroblastoma Group, and the Italian Neuroblastoma Group.

Funding

Grant funding provided by NIH/NCI R37CA262781 (MAA) and R25CA240134 (EN), the Sam Day Foundation (LX), and R21CA259771 (SXS/LX). Sequencing of CRISPR libraries was performed at the University of Chicago Sequencing Core, which is supported by P30CA014599.

Ethics Statement

Approval of the research protocol by an Institutional Reviewer Board: Yes, UTSW Medical Center.

Consent

The authors have nothing to report.

Conflicts of Interest

The authors declare no conflicts of interest.

References

1. D. Hanahan and R. A. Weinberg, "Hallmarks of Cancer: The Next Generation. Research Support, N.I.H., Extramural Review," *Cell* 144, no. 5 (2011): 646–674, https://doi.org/10.1016/j.cell.2011.02.013.

2. J. M. Heuckmann and R. K. Thomas, "A New Generation of Cancer Genome Diagnostics for Routine Clinical Use: Overcoming the Roadblocks to Personalized Cancer Medicine," *Annals of Oncology* 26, no. 9 (2015): 1830–1837, https://doi.org/10.1093/annonc/mdv184.

3. J. K. Sicklick, S. Kato, R. Okamura, et al., "Molecular Profiling of Cancer Patients Enables Personalized Combination Therapy: The I-PREDICT Study," *Nature Medicine* 25, no. 5 (2019): 744–750, https://doi.org/10.1038/s41591-019-0407-5.

4. G. O. Coyne, N. Takebe, and A. P. Chen, "Defining Precision: The Precision Medicine Initiative Trials NCI-MPACT and NCI-MATCH," *Current Problems in Cancer* 41, no. 3 (2017): 182–193, https://doi.org/10.1016/j.currproblcancer.2017.02.001.

5. "Children Successfully Matched to Therapies," *Cancer Discovery* 9, no. 7 (2019): Of3, https://doi.org/10.1158/2159-8290.Cd-nb2019-059.

6. A. Zehir, R. Benayed, R. H. Shah, et al., "Mutational Landscape of Metastatic Cancer Revealed From Prospective Clinical Sequencing of 10,000 Patients," *Nature Medicine* 23, no. 6 (2017): 703–713, https://doi.org/10.1038/nm.4333.

7. M. Schwaederle, M. Zhao, J. J. Lee, et al., "Association of Biomarker-Based Treatment Strategies With Response Rates and Progression-Free Survival in Refractory Malignant Neoplasms: A Meta-Analysis," *JAMA Oncology Oncol* 2, no. 11 (2016): 1452–1459, https://doi.org/10.1001/jamaoncol.2016.2129.

8. E. Ward, C. DeSantis, A. Robbins, B. Kohler, and A. Jemal, "Childhood and Adolescent Cancer Statistics, 2014," *CA: a Cancer Journal for Clinicians* 64, no. 2 (2014): 83–103, https://doi.org/10.3322/caac.21219.

9. J. M. Maris and K. K. Matthay, "Molecular Biology of Neuroblastoma," *Journal of Clinical Oncology* 17, no. 7 (1999): 2264–2279, https://doi.org/10.1200/JCO.1999.17.7.2264.

10. S. N. Gröbner, B. C. Worst, J. Weischenfeldt, et al., "The Landscape of Genomic Alterations Across Childhood Cancers," *Nature* 555, no. 7696 (2018): 321–327, https://doi.org/10.1038/nature25480.

11. Y. P. Mosse, M. Laudenslager, L. Longo, et al., "Identification of ALK as a Major Familial Neuroblastoma Predisposition Gene," *Research Support, N.I.H., Extramural Research Support, Non-U.S. Govt. Nature* 455, no. 7215 (2008): 930–935, https://doi.org/10.1038/nature07261.

12. M. Sausen, R. J. Leary, S. Jones, et al., "Integrated Genomic Analyses Identify ARID1A and ARID1B Alterations in the Childhood Cancer Neuroblastoma," *Nature Genetics* 45, no. 1 (2013): 12–17, https://doi.org/10.1038/ng.2493.

13. M. S. Irwin, A. Naranjo, F. F. Zhang, et al., "Revised Neuroblastoma Risk Classification System: A Report From the Children's Oncology Group," *Journal of Clinical Oncology* 39, no. 29 (2021): 3229–3241, https://doi.org/10.1200/jco.21.00278.

14. E. F. Attiyeh, W. B. London, Y. P. Mossé, et al., "Chromosome 1p and 11q Deletions and Outcome in Neuroblastoma," *New England Journal of Medicine* 353, no. 21 (2005): 2243–2253, https://doi.org/10.1056/NEJMoa052399.

15. K. R. Bosse and J. M. Maris, "Advances in the Translational Genomics of Neuroblastoma: From Improving Risk Stratification and Revealing Novel Biology to Identifying Actionable Genomic Alterations," *Cancer* 122, no. 1 (2016): 20–33, https://doi.org/10.1002/cncr.29706.

16. J. M. Maris, M. D. Hogarty, R. Bagatell, and S. L. Cohn, "Neuroblastoma," *Lancet* 369, no. 9579 (2007): 2106–2120, https://doi.org/10.1016/s0140-6736(07)60983-0.

17. R. Louhimo, T. Lepikhova, O. Monni, and S. Hautaniemi, "Comparative Analysis of Algorithms for Integration of Copy Number and Expression Data," *Nature Methods* 9, no. 4 (2012): 351–355, https://doi.org/10.1038/nmeth.1893.

18. L. Xu, Y. Zheng, J. Liu, et al., "Integrative Bayesian Analysis Identifies Rhabdomyosarcoma Disease Genes," *Cell Reports* 24, no. 1 (2018): 238–251, https://doi.org/10.1016/j.celrep.2018.06.006.

19. S. X. Skapek, A. Ferrari, A. A. Gupta, et al., "Rhabdomyosarcoma," *Nature Reviews. Disease Primers* 5, no. 1 (2019): 1, https://doi.org/10.1038/s41572-018-0051-2.

20. S. L. Volchenboum, S. M. Cox, A. Heath, A. Resnick, S. L. Cohn, and R. Grossman, "Data Commons to Support Pediatric Cancer Research," *American Society of Clinical Oncology Educational Book* 37 (2017): 746–752, https://doi.org/10.1200/EDBK_175029.

21. S. Balyasny, S. M. Lee, A. V. Desai, et al., "Association Between Participation in Clinical Trials and Overall Survival Among Children With Intermediate- or High-Risk Neuroblastoma," *JAMA Network Open* 4, no. 7 (2021): e2116248, https://doi.org/10.1001/jamanetworkopen.2021.16248.

22. C. H. Mermel, S. E. Schumacher, B. Hill, M. L. Meyerson, R. Beroukhim, and G. Getz, "GISTIC2.0 Facilitates Sensitive and Confident Localization of the Targets of Focal Somatic Copy-Number Alteration in Human Cancers," *Genome Biology* 12, no. 4 (2011): R41, https://doi.org/10.1186/gb-2011-12-4-r41.

23. M. Martin, "Cutadapt Removes Adapter Sequences From High-Throughput Sequencing Reads," *EMBnet.Journal* 17, no. 1 (2011): 10–12.

24. D. Kim, J. M. Paggi, C. Park, C. Bennett, and S. L. Salzberg, "Graph-Based Genome Alignment and Genotyping With HISAT2 and HISAT-Genotype," *Nature Biotechnology* 37, no. 8 (2019): 907–915, https://doi.org/10.1038/s41587-019-0201-4.

25. M. I. Love, W. Huber, and S. Anders, "Moderated Estimation of Fold Change and Dispersion for RNA-Seq Data With DESeq2," *Genome Biology* 15, no. 12 (2014): 550, https://doi.org/10.1186/s13059-014-0550-8.

26. J. K. Kruschke, "Bayesian Estimation Supersedes the t Test," *Journal of Experimental Psychology. General* 142, no. 2 (2013): 573–603, https://doi.org/10.1037/a0029146.

27. J. K. Kruschke and T. M. Liddell, "The Bayesian New Statistics: Hypothesis Testing, Estimation, Meta-Analysis, and Power Analysis From a Bayesian Perspective," *Psychonomic Bulletin & Review* 25, no. 1 (2018): 178–206, https://doi.org/10.3758/s13423-016-1221-4.

28. A. Gelman, J. Carlin, H. Stern, D. Dunson, A. Vehtari, and D. Rubin, *Bayesian data analysis* (Chapman and Hall-CRC press, 2014).

29. O. Shalem, N. E. Sanjana, E. Hartenian, et al., "Genome-Scale CRISPR-Cas9 Knockout Screening in Human Cells," *Science* 343, no. 6166 (2014): 84–87, https://doi.org/10.1126/science.1247005.

30. S. Chen, N. E. Sanjana, K. Zheng, et al., "Genome-Wide CRISPR Screen in a Mouse Model of Tumor Growth and Metastasis," *Cell* 160, no. 6 (2015): 1246–1260, https://doi.org/10.1016/j.cell.2015.02.038.

31. J. A. Meier, F. Zhang, and N. E. Sanjana, "GUIDES: sgRNA Design for Loss-Of-Function Screens," *Nature Methods* 14, no. 9 (2017): 831–832, https://doi.org/10.1038/nmeth.4423.

32. W. Li, H. Xu, T. Xiao, et al., "MAGeCK Enables Robust Identification of Essential Genes From Genome-Scale CRISPR/Cas9 Knockout Screens," *Genome Biology* 15, no. 12 (2014): 554, https://doi.org/10.1186/s13059-014-0554-4.

33. DepMap B, "DepMap 24Q4 Public. Figshare + Dataset," (2024).

34. Y. Zheng, Y. D. Zhao, M. Gibbons, et al., "Tgfbeta Signaling Directly Induces Arf Promoter Remodeling by a Mechanism Involving Smads 2/3 and p38 MAPK," *Journal of Biological Chemistry* 285, no. 46 (2010): 35654–35664, https://doi.org/10.1074/jbc.M110.128959.

35. I. Janoueix-Lerosey, G. Schleiermacher, E. Michels, et al., "Overall Genomic Pattern Is a Predictor of Outcome in Neuroblastoma," *Journal of Clinical Oncology* 27, no. 7 (2009): 1026–1033, https://doi.org/10.1200/JCO.2008.16.0630.

36. G. Schleiermacher, I. Janoueix-Lerosey, A. Ribeiro, et al., "Accumulation of Segmental Alterations Determines Progression in Neuroblastoma," *Journal of Clinical Oncology* 28, no. 19 (2010): 3122–3130, https://doi.org/10.1200/jco.2009.26.7955.

37. Y. P. Mosse, S. J. Diskin, N. Wasserman, et al., "Neuroblastomas Have Distinct Genomic DNA Profiles That Predict Clinical Phenotype and Regional Gene Expression," *Genes, Chromosomes & Cancer* 46, no. 10 (2007): 936–949, https://doi.org/10.1002/gcc.20477.

38. A. J. Aguirre, R. M. Meyers, B. A. Weir, et al., "Genomic Copy Number Dictates a Gene-Independent Cell Response to CRISPR/Cas9 Targeting," *Cancer Discovery* 6, no. 8 (2016): 914–929, https://doi.org/10.1158/2159-8290.CD-16-0154.

39. K. Lin, Y. C. Chang, M. Billmann, et al., "A Scalable Platform for Efficient CRISPR-Cas9 Chemical-Genetic Screens of DNA Damage-Inducing Compounds," *Scientific Reports* 14, no. 1 (2024): 2508, https://doi.org/10.1038/s41598-024-51735-y.

40. K. K. Matthay, J. M. Maris, G. Schleiermacher, et al., "Neuroblastoma," *Nature Reviews. Disease Primers* 2 (2016): 16078, https://doi.org/10.1038/nrdp.2016.78.

41. P. Depuydt, V. Boeva, T. D. Hocking, et al., "Genomic Amplifications and Distal 6q Loss: Novel Markers for Poor Survival in High-Risk Neuroblastoma Patients," *Journal of the National Cancer Institute* 110, no. 10 (2018): 1084–1093, https://doi.org/10.1093/jnci/djy022.

42. G. Schleiermacher, V. Mosseri, W. B. London, et al., "Segmental Chromosomal Alterations Have Prognostic Impact in Neuroblastoma: A Report From the INRG Project," *British Journal of Cancer* 107, no. 8 (2012): 1418–1422, https://doi.org/10.1038/bjc.2012.375.

43. N. Bown, S. Cotterill, M. Lastowska, et al., "Gain of Chromosome Arm 17q and Adverse Outcome in Patients With Neuroblastoma," *New England Journal of Medicine* 340, no. 25 (1999): 1954–1961, https://doi.org/10.1056/NEJM199906243402504.

44. H. Koyama, T. Zhuang, J. E. Light, et al., "Mechanisms of CHD5 Inactivation in Neuroblastomas," *Clinical Cancer Research* 18, no. 6 (2012): 1588–1597, https://doi.org/10.1158/1078-0432.CCR-11-2644.

45. T. J. Pugh, O. Morozova, E. F. Attiyeh, et al., "The Genetic Landscape of High-Risk Neuroblastoma," *Nature Genetics* 45, no. 3 (2013): 279–284, https://doi.org/10.1038/ng.2529.

46. E. R. Berko, A. Naranjo, A. A. Daniels, et al., "Frequency and Clinical Significance of Clonal and Subclonal Driver Mutations in High-Risk Neuroblastoma at Diagnosis: A Children's Oncology Group Study," *Journal of Clinical Oncology* 43, no. 14 (2025): 1673–1684, https://doi.org/10.1200/jco-24-02407.

47. C. Thirant, A. Peltier, S. Durand, et al., "Reversible Transitions Between Noradrenergic and Mesenchymal Tumor Identities Define Cell Plasticity in Neuroblastoma," *Nature Communications* 14, no. 1 (2023): 2575, https://doi.org/10.1038/s41467-023-38239-5.

48. A. D. Durbin, M. W. Zimmerman, N. V. Dharia, et al., "Selective Gene Dependencies in MYCN-Amplified Neuroblastoma Include the Core Transcriptional Regulatory Circuitry," *Nature Genetics* 50, no. 9 (2018): 1240–1246, https://doi.org/10.1038/s41588-018-0191-z.

49. J. Takita, H. W. Yang, Y. Y. Chen, et al., "Allelic Imbalance on Chromosome 2q and Alterations of the Caspase 8 Gene in Neuroblastoma," *Oncogene* 20, no. 32 (2001): 4424–4432, https://doi.org/10.1038/sj.onc.1204521.

50. Z. Zhou, Q. Gong, Y. Wang, Y. Li, Y. Zhang, and W. Huang, "The Biological Function and Clinical Significance of SF3B1 Mutations in Cancer," *Biomarker Research* 8, no. 1 (2020): 38, https://doi.org/10.1186/s40364-020-00220-5.

51. J. J. Molenaar, J. Koster, D. A. Zwijnenburg, et al., "Sequencing of Neuroblastoma Identifies Chromothripsis and Defects in Neuritogenesis Genes," *Nature* 483, no. 7391 (2012): 589–593, https://doi.org/10.1038/nature10910.

52. K. Suda, L. Rozeboom, H. Yu, et al., "Potential Effect of Spliceosome Inhibition in Small Cell Lung Cancer Irrespective of the MYC Status," *PLoS One* 12, no. 2 (2017): e0172209, https://doi.org/10.1371/journal.pone.0172209.

53. D. P. Steensma, M. Wermke, V. M. Klimek, et al., "Phase I First-In-Human Dose Escalation Study of the Oral SF3B1 Modulator H3B-8800 in Myeloid Neoplasms," *Leukemia* 35, no. 12 (2021): 3542–3550, https://doi.org/10.1038/s41375-021-01328-9.

54. K. M. Lappin, E. M. Barros, S. S. Jhujh, et al., "Cancer-Associated SF3B1 Mutations Confer a BRCA-Like Cellular Phenotype and Synthetic Lethality to PARP Inhibitors," *Cancer Research* 82, no. 5 (2022): 819–830, https://doi.org/10.1158/0008-5472.Can-21-1843.

55. M. Takagi, C. Ogawa, T. Iehara, et al., "First Phase 1 Clinical Study of Olaparib in Pediatric Patients With Refractory Solid Tumors," *Cancer* 128, no. 15 (2022): 2949–2957, https://doi.org/10.1002/cncr.34270.

56. J. L. Reiter and G. M. Brodeur, "MYCN Is the Only Highly Expressed Gene From the Core Amplified Domain in Human Neuroblastomas," *Genes, Chromosomes & Cancer* 23, no. 2 (1998): 134–140, https://doi.org/10.1002/(sici)1098-2264(199810)23:2<134::aid-gcc6>3.0.co;2-3.

57. B. Galinski, M. Luxemburg, Y. Landesman, et al., "XPO1 Inhibition With Selinexor Synergizes With Proteasome Inhibition in Neuroblastoma by Targeting Nuclear Export of IkB," *Translational Oncology* 14, no. 8 (2021): 101114, https://doi.org/10.1016/j.tranon.2021.101114.

58. R. Nguyen, H. Wang, M. Sun, D. G. Lee, J. Peng, and C. J. Thiele, "Combining Selinexor With Alisertib to Target the p53 Pathway in Neuroblastoma," *Neoplasia* 26 (2022): 100776, https://doi.org/10.1016/j.neo.2022.100776.

59. A. L. Green, C. G. Minard, X. Liu, et al., "Phase I Trial of Selinexor in Pediatric Recurrent/Refractory Solid and CNS Tumors (ADVL1414): A Children's Oncology Group Phase I Consortium Trial," *Clinical Cancer Research* 31, no. 9 (2025): 1587–1595, https://doi.org/10.1158/1078-0432.Ccr-24-2754.

Supporting Information

Additional supporting information can be found online in the Supporting Information section. **Figure S1:** Diagram depicting the four computational steps in the iExCN analysis. Code is available at https://github.com/Lin-Xu-lab/iExCN. **Figure S2:** There are no significant differences in the number of genes with copy number (CN) gains or losses in neuroblastoma cases with and without MYCN gains. These data were generated from 195 GMKF specimens: 22 were MYCN-amplified and 173 had no MYCN-amplification. **Figure S3:** Descriptive analysis of

CN gains in iExCN candidates across the analyzed cohort shows (A) Graphical representation of the CN gains in each case shows that the number of iExCN-nominated oncogenes harboring CN gains is similarly distributed across low, intermediate, and high-risk groups. Of note, 23 cases showed no CN gains in any iExCN genes. (B) Chart shows the average (and standard deviation) of CN gains in each of the iExCN genes; and (C) the number of cases with detectable gains of each iExCN gene. The 201 unique GMKF cases in this analysis included the 195 cases with both gene copy-number and gene-expression data, plus 6 additional cases contributing copy-number that were not part of the paired CN/expression iExCN discovery subset. **Figure S4:** DepMap dependency scores in Kelly, SK-N-AS, and SK-N-SH, from which SHEP cells were derived. **Figure S5:** Targeting of iExCN-nominated oncogenes (DDX5, MDM4, PPM1D, KAT7, FUBP1, TRRAP, and HNRNPA2B1) by siRNA depletes expression in Kelly, SHEP, and SK-N-AS cell lines, and impacts cell accumulation at 3 and 6 days. Cell accumulation was assessed using the CyQuant assay. Graphs are of a single experiment with six biological replicates per group. $****=p<0.0001$, $**=p<0.01$, as measured by a two-tailed unpaired t-test. **Figure S6:** In aggregate, iExCN genes show significant negative DepMap dependency scores across a panel of 34 neuroblastoma cell lines. Negative control genes are randomly chosen from all genes expressed in neuroblastoma specimens (A) and positive control genes are known to be essential in mammalian cells. Significance was assessed by $p<2\times10-16$; ANOVA with Tukey's post hoc test. **Figure S7:** Box plots show average DepMap dependency scores in 34 neuroblastoma cases for randomly chosen, negative control genes (A) and positive control genes that are known to be essential in mammalian cells (B). (See more details in Methods). **Table S1:** sgRNA sequences for the iExCN mini-pool targeting iExCN (green), positive control (light blue) and negative controls (peach) genes. **Table S2:** Oligonucleotide sequences for molecular biology. **Table S3:** iExCN Scores for top-ranking genes. **Table S4:** Pathways significantly enriched in iExCN genes. **Table S5:** Chromosomal location of iExCN genes. **Table S6:** Co-occurring copy number increases in iExCN-nominated genes. **Table S7:** Distribution of MYCN amplification in high-risk patients from the GMKF and TARGET datasets.